AAS 99-013

Experimental Results on Three Multipath Compensation Techniques for GPS-based Attitude Determination

Alessandro Pasetti and Luisella Giulicchi

European Space Agency, ESA-Estec

21st ANNUAL AAS GUIDANCE AND CONTROL CONFERENCE

February 3-7, 1999
Breckenridge, Colorado

Sponsored by
Rocky Mountain Section

AAS Publications Office, P.O. Box 28130 - San Diego, California 92198

AAS 00-013

EXPERIMENTAL RESULTS ON THREE MULTIPATH COMPENSATION TECHNIQUES FOR GPS-BASED ATTITUDE DETERMINATION*

Alessandro Pasetti† and **Luisella Giulicchi**‡

Theoretical analyses supported by simulation and test results indicate that GPS-based attitude determination can yield accuracy of 0.5 to 1 deg. The limiting factor in the achievable accuracy is the multipath error, which arises when the GPS signal is reflected or diffracted by surfaces around the antenna. This paper considers three multipath compensation techniques. All three techniques can be implemented in the GPS receiver software. Their effectiveness was verified on a GPS test facility consisting of a tilt table with two degrees of freedom supporting a baseline of 1 m in length with two antennas connected to a commercial GPS receiver modified to process differential phase measurements. The first technique compensates multipath using a look-up table that stores the expected multipath error as a function of the azimuth and elevation angles of the incoming GPS signal. The second technique treats the multipath component of the attitude estimation error as a stationary correlated (colored) noise and uses a Kalman Filter to remove it. The third technique relies on signal-to-noise measurements to compensate multipath effects.

INTRODUCTION

The use of GPS for attitude determination on-board a satellite is by now a well-established technique. It is described in several journal and conference publications and has been the object of at least three major ESA studies (ref. 2, 3 and 4). The principle of GPS-based attitude determination is illustrated in figure 1.

Two GPS antennas are placed at the two ends of a baseline **b**. They are connected to two different channels of the same GPS receiver. The channels are made to track the same GPS satellite. The difference in the measurement of the GPS carrier between the two antennas is proportional to the projection of the baseline vector **b** onto the direction of arrival of the GPS signal. If **s** designates the unitary vector along this direction of arrival, then one can write:

$$\underline{b} \bullet \underline{s} = m\,l + \Delta j + \Delta j_{rn} + \Delta j_{bias} + \Delta j_{mp}$$

* Prepared for technical papers that may later be published in the proceedings of the American Astronautical Society.

† Control Systems Engineer, European Space Agency, Estec, PO Box 299, 2200 AG Noordwijk, The Netherlands, Phone: ++31-71-5655161, Fax: ++31-71-5655432, Email: apasetti@estec.esa.nl.

‡ Control Systems Engineer, European Space Agency, Estec, PO Box 299, 2200 AG Noordwijk, The Netherlands, Phone: ++31-71-5655652, Fax: ++31-71-5655432, Email: lgiulicc@estec.esa.nl.

The phase difference between the two antennas is shown as an integer number m of carrier wavelengths λ, plus the fractional part $\Delta\varphi$, plus measurement errors. The first error term, $\Delta\varphi_{rn}$, is the receiver noise introduced by the receiver tracking loop. This error has the characteristics of white noise with standard deviation of, typically, between 2 and 3 mm of phase*. The second error term, $\Delta\varphi_{bias}$, is the bias error due to an imperfect knowledge of baseline length and of differential line biases in the GPS receiver. In this project, biases were nearly completely removed through a self-survey. Finally, $\Delta\varphi_{mp}$ is the multipath noise. Its size varies widely and can easily exceed 1 centimeter. Its statistical character is that of a strongly correlated (colored) noise.

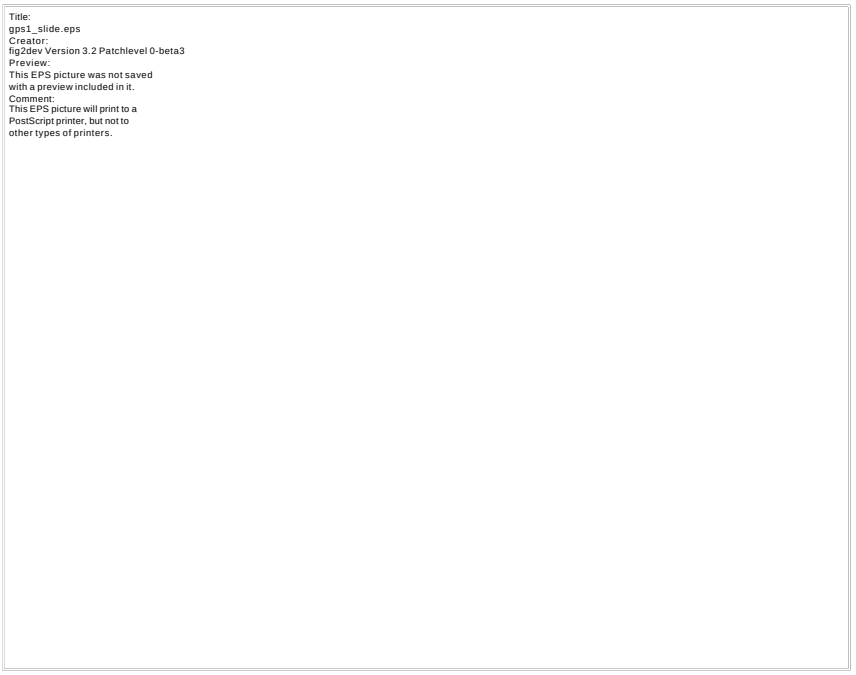

Figure 1: Principle of GPS-based attitude determination

Figure 2 shows a typical sequence of differential carrier phase errors. One can recognize a high-frequency component due to receiver noise and a low-frequency component due to multipath.

* Carrier phase values are normally expressed either in degrees of phase or in millimeters. Since the GPS L1 carrier wavelength is 19 cm, the factor of conversion from millimeters to phase degrees is: 1 mm = 0.53 deg.

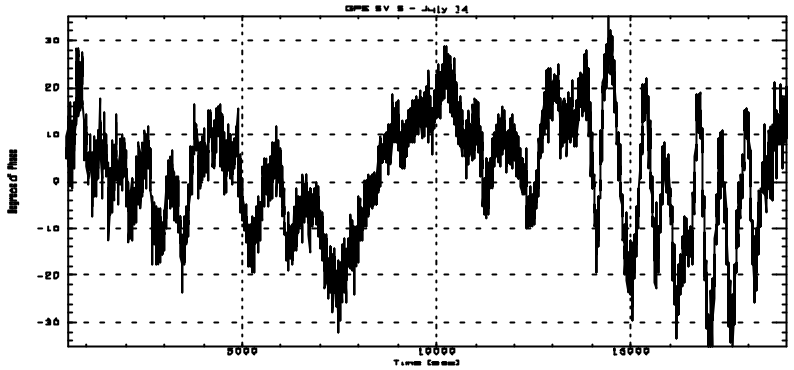

Figure 2: Plot of differential phase error

Figure 3 shows how multipath arises. The signal seen by each antenna is a combination of the direct signal with reflected/diffracted signals. Since multipath depends on the antenna gain pattern and on the geometry of surfaces around the antennas, it is very difficult to predict and hence to compensate.

Fig. 3: Origin of the multipath error

Multipath can be mitigated either with hardware countermeasures (e.g. use of narrow beam antennas, placement of antennas far from reflectors, good rejection of RHP signals, etc.) or through software processing that removes the multipath error. At the software/processing level, multipath mitigation techniques can use either measurement redundancy or error predictability. Measurement redundancy refers to the fact that in order to determine the attitude, measurements from only two GPS satellites are required, but the number of actual measurements available is generally larger. The extra measurements can be used to reduce the error. Processing the measurements with a least-square algorithm usually does this.

This paper considers three software-based multipath-reduction methods that exploit three different kinds of predictability of the multipath error. Multipath is predictable in a first sense because, being a (complex) function of the direction of arrival of the GPS signal, it has a deterministic character. It is therefore in principle possible to pre-compute it and then subtract it

from the differential phase measurements. Secondly, multipath can be seen as partially predictable in a stochastic sense: its associated error can be interpreted as a measurement noise with a strong correlation over time periods of tens or hundreds of seconds - and correlation implies predictability. Finally, since multipath phenomena affect both the phase and the amplitude of the signal, signal power measurements can be used as proxies for measurements of multipath-induced phase errors.

EXPERIMENTAL SET-UP

The results presented in this paper are based on data collected on the Estec GPS Test Facility (GTS for short). The GTS consists of a tilt table, a GPS receiver and a Sun workstation for data processing.

Figure 4: Photo of GTS

The tilt table is a 2-axis medium accuracy table for attitude tests. For this project, it supported an X-shaped structure on which two GPS antennas were mounted at a nominal distance of 1 m. The tilt table was placed under a radome transparent to RF radiation at the L1 wavelength. The tilt table was located on a roof as far away from the obstacles that could be potential sources of multipath as practical. Figure 4 shows the GTS. A wall (not shown in the figure) is on the right side of the table radome at a distance of about 7.5 m. It is covered in plastic sheets, its internal structure is presumably metallic. The parapet at the edge of the roof is about 2.2. m away from the radome and about 0.95 m high. It is therefore below the plane of the antennas (which are at about 1.3 m from the ground). A lightning rod (not shown in the figure) was placed at 0.6 m from the radome. The antenna support structure (shown in figure 5) is made of carbon fiber. The motor casing underneath and the structure supporting the motor are instead mainly metallic.

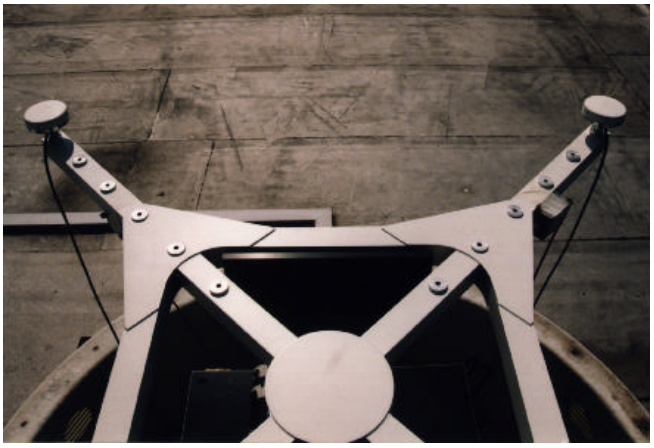

Fig. 5: Photo of GTS antennas and support structure

The GPS receiver is a modified version of the GPS Builder-2 system. This is a commercial receiver available from GEC-Plessey (UK) consisting of a PC board on which one GP2010 and one GP2020 chip are mounted. The GP2010 chip acts as an RF front end to the GP2020 chip which implements 12 L1 correlator channels. For this project, the factory configuration was modified to allow processing data from two antennas.

The test configuration was not meant to reproduce conditions on a satellite. It is however representative in the sense that multipath errors obtained by measurements on a satellite mock-up (ref. 3) and by simulations (ref. 5) are, in terms of amplitude and frequency of variation, similar to those obtained in this project. In any case, the purpose of this project was to demonstrate a concept: to show that the proposed techniques yield accuracy improvement in the particular configuration in which they were tested and that therefore similar improvements can be expected in different configurations. Obviously precise performance assessments remain configuration specific.

MULTIPATH BIAS COMPENSATION

Multipath bias compensation exploits the predictability of the multipath error as a function of the direction of the GPS signal[‡].

The multipath compensation function was represented as a look-up table. Each entry of the table consisted of an azimuth and elevation interval, identifying a set of arrival directions, and of the multipath compensation value for those directions. An alternative approach would have been to represent the multipath function by means of a series of polynomial and/or harmonic terms. This approach is attractive because the specification of the approximation function requires less memory than the specification of a look-up table. However, the plots of the differential phase measurements indicate that multipath varies so rapidly and so irregularly that a good fit would have required a series with a prohibitive number of terms.

[‡] The work described in this section is presented in greater detail in ref. 6.

The look-up table can be visualized by imagining a hemisphere centered on the GPS antennas with its normal aligned with the antenna boresight. A network of latitude lines is then superimposed on the hemisphere. Each latitude band is divided into cells with sides parallel to longitude lines. A grid is thus made up of cells with sides parallel to latitude and longitude lines. Each cell of the grid represents a set of directions of arrival of GPS signals and to each cell is associated a multipath compensation value (e.g. an entry in the look-up table).

It is often stated that multipath is stronger at low elevation and very low near the antenna zenith[†]. If this were so, it would make sense to have a grid with non-uniform mesh size: finer meshing at low elevation (where multipath errors are larger and faster varying) and grosser meshing at high elevation (where multipath errors are smaller and more slowly varying). In fact, the multipath data collected in this project do not show a strong dependency on the elevation (at least not for elevation larger than 20-30 degrees). Furthermore, a grid with uniformly spaced cells makes searches through the look-up table simpler and faster and minimizes the memory required to represent the table (if unequal meshes are used, information about the mesh size has to be stored). For these reasons, a grid of uniform mesh size was used.

The cell size depends on the velocity of variation of multipath errors with respect to the direction of arrival of the GPS signal. Small cells give high accuracy but also require more memory to store the look-up table. In this project, it was found that in order to keep the average change in multipath compensation values across adjacent cells below 10 degrees, it was necessary to have a cell size of 1 deg by 1 deg.

The look-up table was constructed from four days of GTS data, collected with the tilt table in a fixed attitude. The raw differential phase measurements contained both the receiver noise and multipath errors. The former was removed by passing the data through a zero-phase FIR filter with a cut-off frequency of 0.01 Hz. The look-up table was then used to compensate the multipath error on an independent 24-hour data collection. Figure 7 shows the effect of the compensation on one GPS SV.

[†] This statement is often based on simulation results. Preliminary results from an on-going ESA study indicate that simulations underestimate multipath errors for directions close to the zenith. In a second on-going ESA study, simulations to characterize multipath on the Argentinean satellite SAGC indicate the multipath amplitude is roughly uniform for all directions of arrival above 20 deg (NB The satellite carries an 8 m boom).

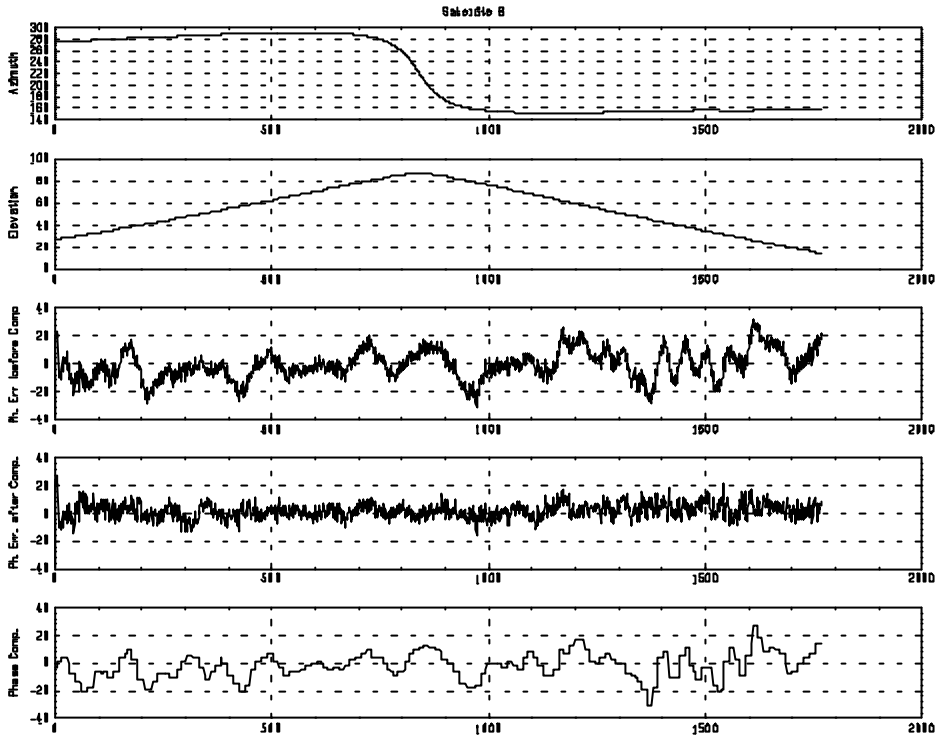

Figure 7: Plot of multipath errors before and after bias compensation

Error Budget

Figure 7 shows that application of multipath compensation has two effects: it reduces the error level and it makes the residual error "whiter" (i.e. closer to a purely random noise). The standard deviation of the differential phase error decreases from 10.8 deg to 6.1 deg (44%). In fact, since compensation is more effective at high elevation, if only elevations above, for example, 30 deg were considered the factor of reduction would be even larger. At 6 deg, the residual error is roughly equal to the standard deviation of the receiver noise, which indicates that compensation has removed the multipath component of the error almost completely.

The residual error, being nearly white, can be further reduced by filtering. Its effectiveness depends on the complexity of the filter. At one extreme, a sophisticated, Kalman-like filter including modeling of the baseline dynamics, might reduce the noise level by a factor 5. At the other extreme, simple filtering relying only on oversampling of the measurements might deliver a reduction factor of 2.

Multipath correction as applied above assumes an *a priori* knowledge of the baseline attitude, which is required to derive the correct compensation factor from the look-up table. In reality, before compensation, the baseline attitude is only approximately known and, given the small mesh size, it is consequently possible that an incorrect correction factor is applied (i.e. that the correction factor from the "wrong" cell is used). The impact of this error can be roughly estimated as described below.

The initial (pre-compensation) error on the differential carrier phase is 10.8 deg (1σ). Assuming a baseline length of 1 m and an ADOP of 1.2, this translates into a baseline attitude error of 1.0 deg (3σ). Since the grid mesh size is 1 deg, one can assume, in a first rough approximation, that the error due to poor knowledge of the attitude results in an error of at most one grid cell. Hence, the multipath reduction factor will, on average, be affected by an error equal to the mean difference between the content of one grid cell and that of its immediate neighbours. In the case at hand, the contents of adjacent grid cells were found to differ, on average, by 8.8 deg of phase. If one assumes that an erroneous grid cell is used 50% of the time, the impact on the error budget is 4.4 deg. The complete error budget is:

1	**Error before compensation**	10.8 deg
2	**Error after compensation**	6.1 deg
3	**Error after filtering of white noise (reduction factor of 2)**	3.1 deg
4	**Error due to uncertainty on initial attitude estimate**	4.4 deg
5	**Total Error (quadratic sum of items 3 and 4)**	5.4 deg

The error due to uncertainty in the initial attitude estimate accounts for a large part of the total error. Consequently ways were investigated to reduce it. An iterative procedure was considered where the attitude at each step is used to estimate multipath correction factors and hence a new, hopefully more accurate, attitude estimate. More precisely:

1. The first baseline attitude estimate is derived from the raw, uncompensated, differential carrier phase measurements.
2. The direction of arrival (in the baseline reference frame) of the GPS signal is computed.
3. The look-up table is used to derive multipath compensation factors.
4. The compensation is applied to the raw differential carrier phase measurements.
5. A new estimate of the attitude is derived from the compensated measurements.
6. Back to point 2.

This iterative procedure is only useful if it can be proven to converge. Convergence conditions are best expressed in terms of a function: $\underline{dDj} = f(\underline{Dj})$ where $\underline{Dj}$ is the vector of differential carrier phase values and $\underline{dDj}$ is the vector of associated multipath corrections. The function f(.) is constructed as follows. From the differential carrier phase measurements $\underline{Dj}$, the baseline attitude is computed. From the baseline attitude, the direction of the GPS satellites in the baseline reference frame is computed. From the direction of the GPS satellites in the baseline reference frame, the multipath correction factors can be derived (through the look-up table). In ref. 6 it is shown that the proposed iterative procedure converges if the largest eigenvalue of the Jacobian of f(.) is smaller than 1. The form of the Jacobian J^f depends on the configuration of the baseline and of the GPS SV' in view at a given time thus its eigenvalues cannot therefore be computed in advance. However, in ref.6 a simple expression, suitable for on-line computation, is derived for an upper bound on the eigenvalues of J^f. Thus the decision on whether to iterate the multipath corrections can be efficiently taken in real-time.

Variations in Grid Mesh Size

Results presented so far were obtained with a grid mesh size of 1 deg x 1 deg. Tests were done with grids with square meshes of 2 and 4 degrees on a side. Multipath reduction levels on data from one particular satellite (GPS SV 4) were as follows:

	Multipath Error (1-s)
Compensation Grid 1 x 1	5.06 deg
Compensation Grid 2 x 2	6.09 deg
Compensation Grid 4 x 4	7.13 deg
No compensation	9.99 deg

Implementation

Multipath bias compensation requires pre-computation of a compensation grid. In a real mission scenario this could be done either by measurement or by simulation. Measurement on the ground using real GPS signals would be impractical for all but the smallest spacecraft. Measurements using a GPS beacon in an RF test facility would also be impractical because it would be necessary to illuminate the spacecraft with a signal that has a nearly plane wave front (to simulate a signal source at a very large distance). This would require a very large test chamber. Measurement in orbit is feasible but would entail a lengthy commissioning phase. Generation of the multipath compensation grid by simulation is more attractive. Unfortunately, there is some evidence that simulations are unable to deliver the necessary level of accuracy. From figure 8, one can see that an error L in modeling the reflector's position results in a phase error of $2L/\cos\theta$ where θ is the signal incidence angle. Thus even modeling errors of the order of 1 mm can give substantial multipath prediction errors. Indeed, the few studies that compare simulations with measurements find multipath predictions errors that sometimes exceed 5-10 deg of phase.

The correction grid is relative to a specific spacecraft configuration. For a spacecraft having moving appendages (e.g. rotating solar arrays), it would in principle be necessary to build a look-up tables for each position of the moving appendages/solar panels. In practice, reflectors that are at a large distance (relative to the L1 wavelength) from the antennas give rise to a multipath error with a high frequency, which can be removed by filtering. Hence if the GPS antennas are located at a sufficient distance from moving appendages, it may still be possible to use a single look-up table.

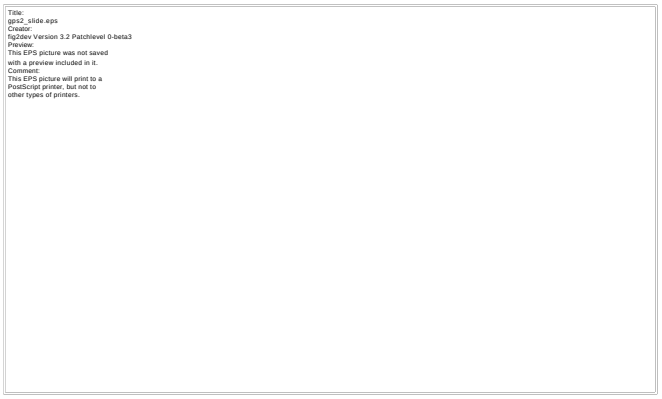

Fig. 8: Phase error as a function of position modeling error

MULTIPATH FREQUENCY COMPENSATION

This is the second of the three methods described in this paper. It exploits the stochastic predictability of the multipath error[†].

A GPS-based attitude determination system can be seen as an algorithm that takes the raw differential phase measurements as inputs and generates an estimate of the baseline attitude as output. If only the latest batch of measurements is used, then the optimal way to estimate the baseline attitude is by least squares. This produces a point estimate that exploits measurement redundancy but does not take account of the past history of measurements. Since it is known that successive measurements of the multipath error are strongly correlated, a point-estimate is wasteful because it does not take advantage of the partial predictability of the measurement error. One way to model this predictability is to treat the stream of measurement errors as a stochastic process.

The treatment of measurement errors as stochastic is correct as far as the receiver noise component of the error is concerned, but it is of course incorrect for the multipath component because multipath errors are deterministic. However, for measurement intervals of limited length, the stream of errors can, with very good approximation, be regarded as stochastic. For analytical treatment to be possible, it is necessary to add the assumption that the stochastic process is stationary.

If the multipath error is regarded as a stationary, discrete stochastic process $\Delta\varphi_{mp}(k)$, then it can be entirely described by its spectral density function $\Delta\vartheta(\omega)$. If it is furthermore assumed that $\Delta\vartheta(\omega)$ is (or can be approximated by) a ratio of polynomials, then $\Delta\varphi_{mp}(k)$ can be seen as being generated by a linear system driven by white noise with zero mean and unitary variance. The transfer function $G_{mp}(z)$ of the linear system must be such that:

[†] The work described in this section is presented in greater detail in ref. 7.

$$G_{mp}\left(e^{jwT}\right) \bullet G_{mp}\left(e^{-jwT}\right) = \Delta J(w)$$

where T is the sampling time. The linear system $G_{mp}(z)$ will be called the "multipath generator" linear system. If the above assumptions hold, each differential phase measurement error can be represented as in figure 8 where $e_{mp}(k)$ is the white noise driving the multipath generator system, $e_{wn}(k)$ is the white noise process accounting for the receiver noise part and $e_{meas}(k)$ is the error on the differential carrier phase.

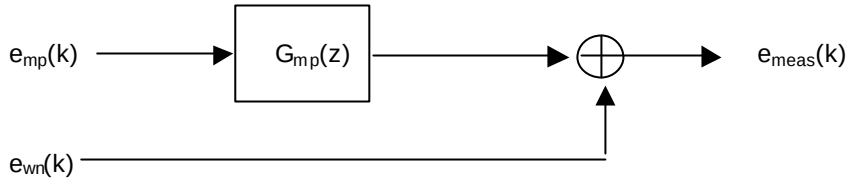

Fig. 9: Multipath generator system

An error model as in figure 9 can be embedded in a model of the spacecraft kinematics and/or dynamics and a Kalman Filter can be used to estimate the multipath error in real-time. This approach was considered but was finally rejected after studying the stationarity of the differential carrier phase error. Figure 2 suggests that the frequency and intensity of multipath vary over time and a power spectral density (PSD) analysis confirmed that the assumption of stationarity does not hold.

An alternative approach was used in this project which uses the point estimates of the attitude as raw measurements rather than the differential phase measurements. Figure 10 shows a plot of the attitude errors. Each point corresponds to a measurement instant and represents the error of the LS attitude estimate obtained at that instant. The attitude error is a function of the errors on the differential phase measurements. The latter have two components, the receiver noise and the multipath noise, with very different frequency signatures. These frequency signatures can be recognized in the figure where one can distinguish a high frequency, white noise-like, component and low frequency components typical of multipath errors.

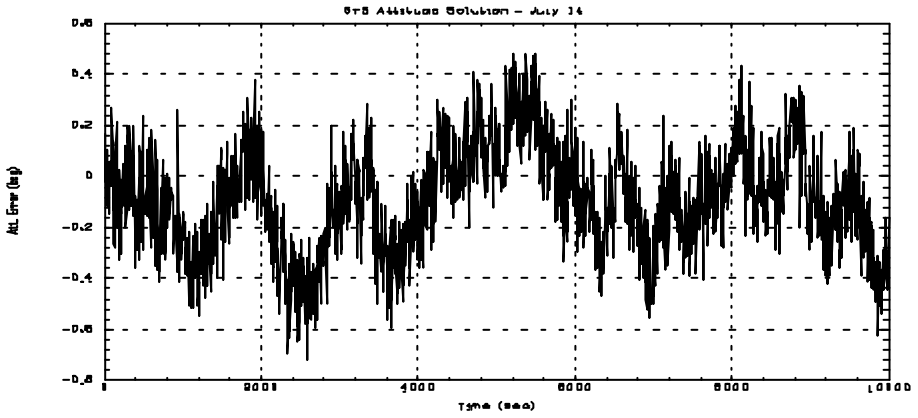

Fig. 10: Euler angle from an LS solution of the attitude

The attitude error can again be seen as a stochastic process. Comparison of figure 10 with figure 2 indicates that the attitude error is more likely to be stationary. Deviations from stationarity for the differential phase errors are related to changes in elevation of the GPS satellites (low elevation satellites cause multipath errors with a higher frequency and a higher intensity than high elevation satellites). One can expect this difference to be mitigated when looking at the attitude error because the latter is obtained as the combination of several (5-6 in the configuration used here) phase measurements from individual satellites whose distribution in the sky is more or less uniform. It is therefore reasonable to expect the attitude error to be more stationary than differential phase errors from individual GPS satellites. This expectation was confirmed by a PSD analysis. Figure 11 shows the PSD of the attitude error computed over four consecutive 6-hour sections of data. The plots are very close together indicating that the spectral characteristics of the attitude solution vary little over time thus supporting the assumption of stationarity.

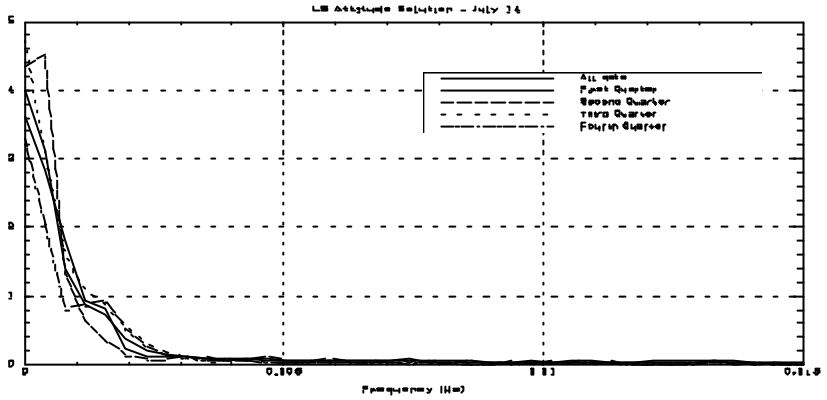

Fig. 11: PSD of consecutive 6-hour segments of attitude error measurements

Having established stationarity, the model of figure 8 can be used with $e_{meas}(k)$ now representing the error on the LS estimate of the attitude. This model was used in a Kalman filter simulation that attempts to estimate (and hence compensate) the multipath component of the attitude error.

Identification of $G_{mp}(z)$

Before simulations could be performed, it was necessary to identify $G_{mp}(z)$. Since the multipath generator linear system is intended for use in a Kalman filter, it is advisable to keep its order low. The simplest option is a first-order lag:

$$G_{mp}(z) = \frac{b_{mp}}{z - a_{mp}}$$

The PSD of its output when driven by white noise of unitary variance is:

$$G_{mp}\left(e^{2\pi j f T}\right) \bullet G_{mp}\left(e^{-2\pi j f T}\right) = \frac{b_{mp}^{\ 2}}{1 + a_{mp}^{\ 2} - 2a_{mp}\cos(2\pi f T)}$$

where T is the filter's sampling time. The shape of this function approximates well that of figure 11. The following values were found to give a good fit between the attitude error PSD and the multipath generator PSD:

$$a_{mp} = 0.98 \quad b_{mp} = 0.044 \text{ deg}$$

Figure 12 shows the attitude error PSD and the multipath generator PSD superimposed. Note that the frequency has been rescaled by factor 14 (this accounts for the fact that the GPS satellite seen from an LEO satellite appears to rotate with a frequency 14 times higher and that therefore multipath-induced errors have correspondingly higher frequency).

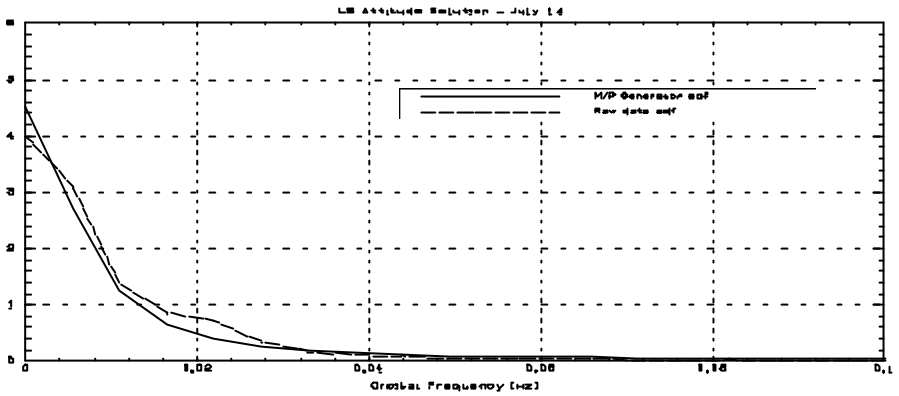

Fig. 12: PSD of multipath generator and of raw attitude error

Simulation Results

The adopted simulation scenario consisted of a satellite model, a measurement model and an estimator model. The satellite model (figure 13) was a single-axis control loop for the satellite attitude (J=200 kg m^2). The attitude controller was a simple PD controller (k_p=10 rad/Nm, k_d=226 1/Nms). The feedback signal was a noisy measurement of the satellite attitude (with noise standard deviation of 0.1 deg). A simple (sinusoidal) torque disturbance was added to simulate the presence of disturbances and inter-axes couplings (with amplitude of 0.01 Nm and frequency of 0.05 Hz).

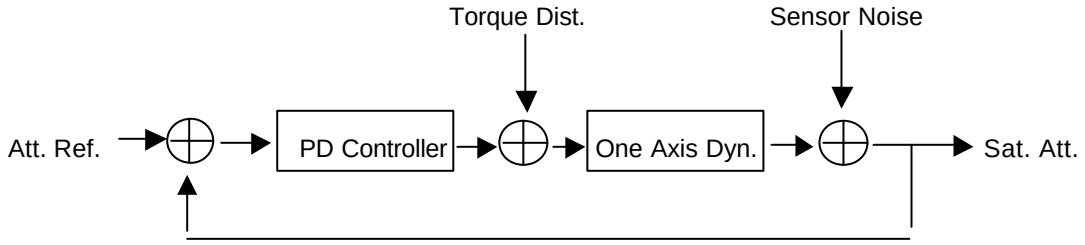

Fig. 13: Satellite model

The measurement model (figure 14) generated raw attitude measurements as the sum of the "true" attitude with an error. The stream of error data taken from real measurements performed on the GTS. It was therefore very representative of real measurement errors.

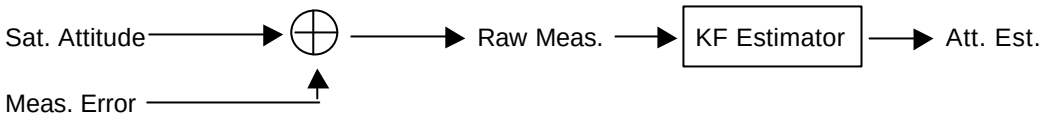

Fig. 14: Measurement and estimator model

The estimator was based on a Kalman filter. Two series of simulations were done. In the first one, a kinematic model of the satellite was used. In the second one, a dynamical model was used. In both cases, a comparison is made between the KF estimate when the error on the raw attitude measurement is treated as a white noise ("Simple KF") and when this error is instead modelled as in figure 9 ("Multipath KF"). The second approach represents the multipath frequency compensation technique advocated here.

Kinematic Estimator: The simple KF used the following models for the satellite attitude and for the measurements:

$$x_{sat}(k+1) = x_{sat}(k) + e_{sat}(k)$$
$$y(k) = x_{sat}(k) + e_{meas}(k)$$

where x_{sat} denotes the satellite attitude and $e_{sat}(k)$ and $e_{meas}(k)$ are the noise on the state and on the measurement. The corresponding estimator is:

$$x^*_{sat}(k+1) = x^*_{sat}(k)(1-k_s) + k_s y(k)$$

where asterisked variables are estimates and k_s is the Kalman. This estimator is suboptimal because it implicitly relies on the assumption that the state and measurement noises are uncorrelated white noises. This is certainly not the case for the measurement noise, which is mainly due to (highly correlated) multipath errors. The multipath KF estimator avoids this shortcoming by modeling the multipath generation process as a first-order process. Its model equations are:

$$\begin{bmatrix} x_{sat}(k+1) \\ x_{mp}(k+1) \end{bmatrix} = \begin{bmatrix} 1 & 0 \\ 0 & a_{mp} \end{bmatrix} \begin{bmatrix} x_{sat}(k) \\ x_{mp}(k) \end{bmatrix} + \begin{bmatrix} 1 & 0 \\ 0 & b_{mp} \end{bmatrix} \begin{bmatrix} e_{sat}(k) \\ e_{mp}(k) \end{bmatrix}$$
$$y(k) = \begin{bmatrix} 1 & 1 \end{bmatrix} \begin{bmatrix} x_{sat}(k) \\ x_{mp}(k) \end{bmatrix} + e_{wn}(k)$$

Now $x_{mp}(k)$ is a variable representing the multipath component of the attitude error. The parameters a_{mp} and b_{mp} define the model of the multipath generator as found in the previous section. The KF estimator for this system of equations is:

$$\begin{bmatrix} x^*_{sat}(k+1) \\ x^*_{mp}(k+1) \end{bmatrix} = \left(\begin{bmatrix} 1 & 0 \\ 0 & a_{mp} \end{bmatrix} - K_{mp} \begin{bmatrix} 1 & 1 \end{bmatrix} \right) \begin{bmatrix} x^*_{sat}(k) \\ x^*_{mp}(k) \end{bmatrix} + K_{mp} y(k)$$

Figure 14 shows the results of the simulations. One can see that the multipath estimator improves the estimate quality by containing the maximum excursions of the estimate error.

The 1 σ estimate errors are:

	Attitude Estimation Error (1 s)
Raw Measurements	0.20 deg
Simple KF	0.16 deg
Multipath KF	0.10 deg

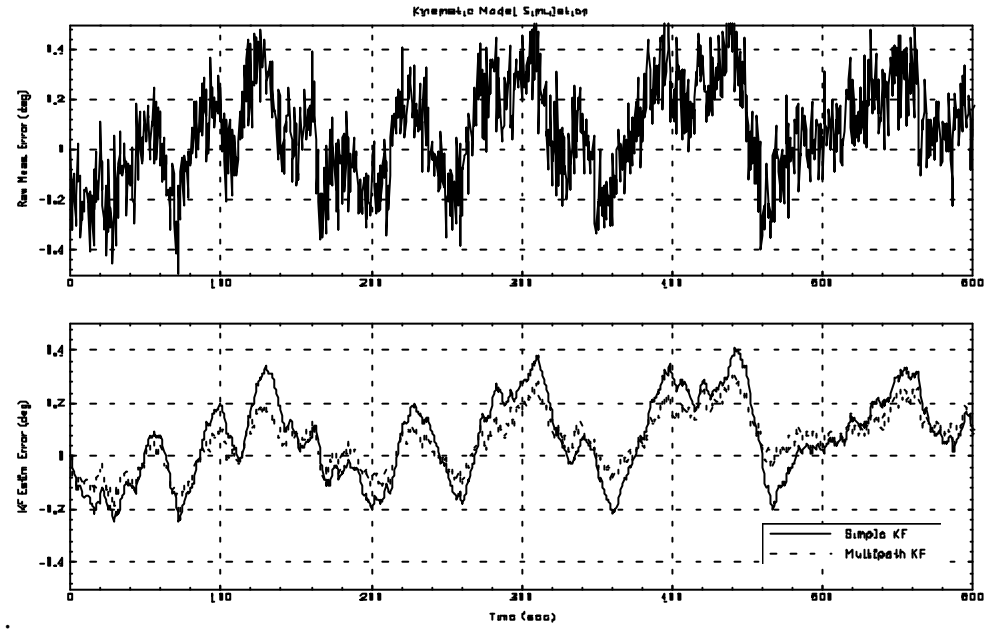

Fig. 15: Simulation results – kinematic case

Dynamical Estimator: The dynamical estimator differed from the kinematic one in using a model of the satellite dynamics. The satellite dynamics was modelled as follows:

$$\underline{x}_{sat}(k) = G_{sat}(z)\big(u(k) + e_{sat}(k)\big) = \frac{T^2(z+1)}{2J(z-1)^2}\big(u(k) + e_{sat}(k)\big)$$

where $\underline{\mathbf{x}}_{sat}(k)$ is the satellite state (angular position and rate), u(k) is the control torque, and $G_{sat}(k)$ is the discretized version of the single-axis satellite transfer function. $G_{sat}(k)$ included a 10% uncertainty in the knowledge of the spacecraft inertia. As in the case of the kinematic model, two types of Kalman filter were tested: the "simple" Kalman filter and the "multipath" Kalman filter. The former models the measurement error as a pure white noise. Its model equations are:

$$\underline{x}_{sat}(k+1) = A_{sat}x_{sat}(k) + B_{sat}u(k) + B_{sat}e_{sat}(k)$$
$$y(k) = C_{sat}\underline{x}_{sat}(k) + e_{meas}(k)$$

where (A_{sat}, B_{sat}, C_{sat}) is a state-space realization of $G_{sat}(k)$. The simple KF estimator consequently is:

$$\underline{x}^*_{sat}(k+1) = A_{sat}\underline{x}^*_{sat}(k) + K_s\left(y(k) - C_{sat}\underline{x}^*_{sat}(k)\right) + B_{sat}u(k)$$

The multipath KF estimator attempts to model the multipath generation process as a first-order process. Its model equations are:

$$\begin{bmatrix}\underline{x}_{sat}(k+1)\\ x_{mp}(k+1)\end{bmatrix} = \begin{bmatrix}A_{sat} & 0\\ 0 & a_{mp}\end{bmatrix}\begin{bmatrix}\underline{x}_{sat}(k)\\ x_{mp}(k)\end{bmatrix} + \begin{bmatrix}B_{sat} & 0\\ 0 & b_{mp}\end{bmatrix}\begin{bmatrix}e_{sat}(k)\\ e_{mp}(k)\end{bmatrix}$$
$$y(k) = \begin{bmatrix}C_{sat} & 1\end{bmatrix}\begin{bmatrix}\underline{x}_{sat}(k)\\ x_{mp}(k)\end{bmatrix} + e_{wn}(k)$$

where a_{mp} and b_{mp} are again the multipath generator model parameters. The associated KF estimator for this system of equations is:

$$\begin{bmatrix}\underline{x}^*_{sat}(k+1)\\ x^*_{mp}(k+1)\end{bmatrix} = \left(\begin{bmatrix}A_{sat} & 0\\ 0 & a_{mp}\end{bmatrix} - K_{mp}\begin{bmatrix}C_{sat} & 1\end{bmatrix}\right)\begin{bmatrix}\underline{x}^*_{sat}(k)\\ x^*_{mp}(k)\end{bmatrix} + K_{mp}y(k)$$
$$j\,(k) = \begin{bmatrix}C_{sat} & 0\end{bmatrix}\begin{bmatrix}\underline{x}^*_{sat}(k)\\ x^*_{mp}(k)\end{bmatrix}$$

where K_{mp} is a vector of gains. The attitude estimation accuracy was:

	Attitude Estimation Error (1 s)
Raw Measurements	0.20 deg
Simple KF	0.12 deg
Multipath KF	0.09 deg

Interestingly, the improvement in going from simple to multipath KF was smaller than in the kinematic model case. Other simulations were done with different values of mismatch between real-world and estimated satellite inertia and of state noise. The relative gain of switching from the simple KF was either unchanged or greater. Greater gains occurred when the fidelity of the model assumed by the KF was degraded and the performance of the KF estimator tended towards that of the kinematic estimator.

SNR MULTIPATH COMPENSATION

This is the third of the three methods described in this paper. It exploits the predictability of the multipath error on the phase from SNR data[†].

[†] The work described in this section is presented in greater detail in ref. 8.

It is convenient to adopt a phasor notation for the GPS signals. The direct signals at the two antennas will then be represented as follows:

$$s_{1d} = A\,e^{jj} = A\angle j$$
$$s_{2d} = A\,e^{j(j+\Delta j)} = A\angle(j+\Delta j)$$

where $\Delta\varphi$ represents the theoretical phase difference (the phase difference that would be observed in the absence of any multipath errors). Reflected signals can be written as:

$$s_{1r} = a_1 A\,e^{j(j+b_1)} = a_1 A\angle(j+b_1)$$
$$s_{2r} = a_2 A\,e^{j(j+\Delta j+b_{21})} = a_2 A\angle(j+\Delta j+b_2)$$

The coefficient α_i is the reflection coefficient. Its value is normally very small (typically below 0.1). The phase angles β_i account for the longer path that the reflected rays have to travel to reach the antennas. In a first approximation, the differential phase and differential amplitudes across the antennas are:

$$\Delta j_{mp} = \angle(s_1 - s_2) - \Delta j = a_1 \sin b_1 - a_2 \sin b_2$$
$$\Delta M = a_1 A\cos b_1 - a_2 A\cos b_2$$

Following ref. 9 and 10, one can hypothesize that the angles β_i have the form:

$$b_i = w_{mp-i}t + f_i$$

where $\omega_{mp\text{-}i}$ expresses the velocity with which the multipath phase is changing. This is a function of the distance of the multipath generating obstacle and of the GPS SV position and its rate of change. Obviously both $\omega_{mp\text{-}i}$ and ϕ_i are time dependent. Consider now the time derivative of ΔM:

$$\Delta M' = -a_1 w_{mp-i} A\sin b_1 + a_2 w_{mp-i} A\sin b_2 + o(A, w_{mp-i}, f, a) \cong -A w_{mp-i}\Delta j_{mp}$$

The function o( ) captures terms that originate from the time-dependence of A, α_i, $\omega_{mp\text{-}i}$, and ϕ. Because these quantities vary more slowly than the angles β_i, it can be neglected leading to the conclusion that *the amplitude of the multipath error is proportional to the derivative of the difference of the signal amplitudes seen at the two antennas*. This relationship potentially gives a very simple way of directly estimating the multipath error. The SNR compensation method consists precisely in using it to compensate the multipath error. The legitimacy of doing so depends on several assumptions of which the most restrictive is the assumption of a single (or at least a dominant) multipath reflector.

The validity of this assumption was tested with 24-hour of measurements from the GTS configuration. The derivative of the differential amplitude at time t_i was computed by LS-fitting a straight line to the differential amplitude measurements in the range [(t_i-100sec), (t_1+100sec)]. The derivative was simply the slope of the straight line. Obviously, this is a non-causal way of computing the derivative. This algorithm, though unsuitable for operational use, is appropriate for an initial assessment of the compensation method.

Plots of the derivative of the differential amplitude were superimposed on the plots of the multipath errors for 11 satellites. One such plot is shown in figure 16. The multipath error was

filtered (zero-phase FIR filter of order 19 with a cut-off frequency of 0.01 Hz). The plot of the derivative of the differential amplitude was scaled so as to be easily comparable to that of the multipath errors. The absolute value of the scaling factor used for the plots was 1600. If the dominant-source assumption were satisfied, the scaling factor would be equal to A ω_{mp}. It should be noted that ω_{mp} can be negative. In fact, it was found that optimal matching of the multipath error to the derivative of the differential amplitude was obtained when a positive scaling coefficient was used where the GPS SV elevation is increasing and a negative scaling factor is used where the elevation is decreasing. The plots were therefore produced with a scaling factor of +1600 for times of increasing elevation and −1600 for times of decreasing elevation.

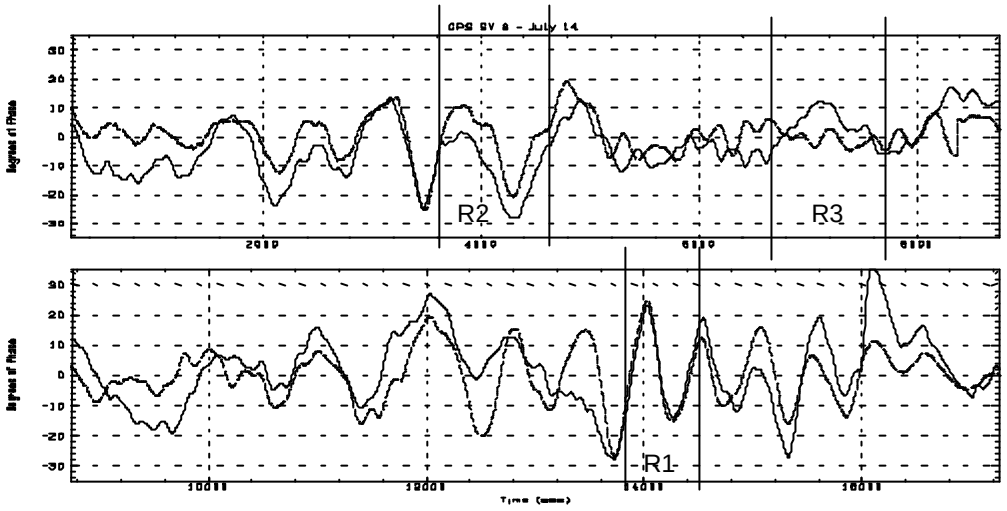

Fig. 17: Derivative of diff. amplitude (dashed line) and of m/p error (solid line)

Figure 17 indicates that the multipath error and the derivative of the differential amplitude are closely related, although the exact nature of the relationship is difficult to capture. Broadly speaking, it is possible to recognize three types of regions in the plots. In r*egion 1* (e.g. R1) there is a very good match between the plot of the multipath error and the plot of the derivative of the differential amplitude. In *region 2* (e.g. R2) the plot of the multipath error and the plot of the derivative of the differential amplitude differ by a constant bias (similar behaviour to region 1 but one plot is shifted up or down with respect to the other). In *region 3* (e.g. R3) there is no apparent relationship between the multipath error and the derivative of the differential amplitude.

Region 1 is where the dominant source hypothesis holds. It is interesting to note that, where region 1 behaviour prevails, the scaling factor between the multipath error and the derivative of the differential amplitude is roughly constant. Overall, region 1 behavior is limited to perhaps 20-30% of the time and seems to be especially strong where the multipath error undergoes large oscillations. Region 2 behavior is something of a puzzle: the theoretical origin of the offset between the two plots is unclear.

The results presented in the figures suggest that, over significant sections of sky, the derivative of the differential amplitude and the multipath error are closely related and that the latter could consequently be estimated from the former. Future work on this method will

investigate the relationship between the derivative of the differential amplitude and the multipath error on a different configuration to ascertain its generality. The problem of obtaining the derivative of the differential amplitude in real-time will also be considered more attentively. Finally, in this project the match between the derivative of the differential amplitude and the multipath level were studied by visual inspections. Algorithms will be developed to automatically identify regions where a relationship of proportionality holds and to estimate the coefficient of proportionality. This information will then be used in a practical multipath correction scheme.

CONCLUSIONS

This paper discussed three multipath compensation methods and, for the first two, tested their effectiveness on measurements collected on an on-ground GPS test facility.

The first method, multipath bias compensation uses a pre-computed model of the multipath error as a function of the azimuth and elevation of the GPS signal to remove the multipath from measurements. The multipath correction function was implemented as a look-up table. Experimental results indicate that, using a granularity of 1 deg for the look-up table, multipath effects can in principle be completely removed leaving only the receiver noise as residual error. This noise, being white, can be further reduced by filtering. An important source of error in this method is the error in the initial estimate of the baseline attitude. An iterative procedure is proposed to remove it and a convergence condition for this procedure is derived.

This method is the one most commonly proposed to compensate multipath. In principle, it promises to be extremely effective. The possibility of applying it iteratively, in particular, could eliminate the multipath error altogether. However, the construction of a finely grained correction grid requires a degree of accuracy in multipath modeling/prediction tools that is probably not achievable in practice.

Kalman filtering (KF) has often been proposed as a way to reduce multipath errors (e.g. in ref. 3 and 4) but it is often applied in a "naïve" manner that treats the multipath error as a white noise. This is wasteful because even a casual look at a multipath noise plot shows it to be highly correlated and hence partially predictable. This project showed that multipath errors, at the level of attitude measurements, can be treated as stationary noise processes generated by a first order linear system driven by white noise. This simple model, if incorporated in the KF, can improve estimation accuracy, with respect to the "naïve KF", by up to 40%. This method has no real shortcomings. At a modest cost – one extra state in a KF – it delivers substantial performance improvements. The two parameters for the multipath model in the KF can be easily estimated by simulation.

The third method, SNR compensation, has a more speculative character. Preliminary results indicate a strong relationship between multipath errors and the derivative of the differential amplitude but more analyses are required to ascertain how often this relationship holds. Tests for this purpose are planned for the first half of next year. If successful, they could open the way to a very simple and very effective means of directly estimating the multipath error in real-time.

REFERENCES

1. C. Cohen, “Attitude Determination Using GPS” *PhD Dissertation, University of Stanford, Dept. of Aeronautics and Astronautics.,* Dec. 1992.
2. GMV, “Study of Autonomous Orbit and Attitude Determination Techniques for Low-Earth Orbit Observation Systems*”, Final Report from Estec Study Contract N. 10976/94/NL/CN*, Nov. 1995.
3. L. Vaillon (MMS-Toulouse), “Attitude Determination using GPS*”, Summary Report from Estec Study Contract 9558/91/NL/JG*, Apr. 1998.
4. Laben, “Spacecraft Attitude Determination using GPS Receiver*”, Phase I Report from Estec Study Contract N. 11805/96/NL/FM*, issue 2, Jan. 1998.
5. Laben, “Spacecraft Attitude Determination using GPS Receiver*”, Estec Study Contract N. 11805/96/NL/FM (Phase II)*, Reports not yet published.
6. L. Giulicchi, A. Pasetti, “GPS Test System Series: Multipath Bias Compensation”, *Estec Report GTS-ES-AP-02,* issue 2, Nov. 1998.
7. A. Pasetti, L. Giulicchi, “GPS Test System Series: Multipath Frequency Compensation”, *Estec Report GTS-ES-AP-03,* issue 2, Sep. 1998.
8. A. Pasetti, L. Giulicchi, “GPS Test System Series: SNR Multipath Compensation”, *Estec Report GTS-ES-AP-04,* issue 1, Nov. 1998.
9. P. Axelrad, C. Comp, P. MacDoran, “Use of Signal-To-Noise Ratio for Multipath Error Correction: Methodology and Experimental Results”, ION GPS-94, Salt Lake City, Sep. 1994
10. C. Comp, P. Axelrad, “An Adaptive SNR-based Carrier Phase Multipath Mitigation Technique”, ION GPS-96, Kansas City, Sep. 1996
11. F. Bernelli-Zazzera, R. Campana, F. Gottifredi, L. Marradi, “GPS Attitude Determination by Kalman Filtering: Simulation of Multipath Rejection”, AAS 98-199, Breckenridge, Feb. 1998